New cubic phase of lithium nitride to 200 GPa

A. Lazicki[1,2], B. Maddox[1,2], W. Evans, C. S. Yoo and A. K. McMahan
[1] *Lawrence Livermore National Laboratory, Livermore, California 94550*

W. E. Pickett and R. T. Scalettar
[2] *Physics Department, University of California, Davis, California 95616*

M. Y. Hu and P. Chow
HPCAT/APS, Argonne National Laboratory, Argonne, Illinois 60439

We present a new cubic γ (Fm3m) Li_3N phase discovered above 40($\pm$5) GPa. Structure and spectral distribution of the cubic phase are examined to 200 GPa with synchrotron x-ray diffraction and inelastic x-ray Raman scattering in a diamond anvil cell. First principles calculations predict a factor-of-five band-gap widening at the onset of the $\beta \rightarrow \gamma$ transition, consistent with an observed color change, and predict metallization at $\sim$8 TPa. The high structural stability, wide band-gap and simple electronic structure of γ-Li_3N are analogous to those of lower valence closed-shell solids including NaCl, MgO and Ne, meriting its use as a low-Z internal pressure standard.

Nitrides are some of the most stable known forms of solids, with chemical bonding ranging from covalent to ionic to semimetallic. Lithium nitride is the only known stable alkali metal nitride and is one of the most ionic of all known nitrides. At ambient pressure, the nitrogen exists in an anomalous multiply charged (nearly N^{3-}) state [1, 2] which is stable only because of its crystal environment - a hexagonal bipyramid of Li^+ ions. This layered structure (α-Li_3N, P6/mnm) consists of Li_2N layers, widely separated and connected by one lithium atom per unit cell occupying a site between the nitrogen atoms in adjacent layers [3, 4]. This material is a superionic conductor via vacancy-induced Li^+ diffusion in the Li_2N layers. [5–7] Its potential for use as an electrolyte in lithium batteries [4], a hydrogen storage medium [8–11] and a component in the synthesis of GaN [12] has prompted several studies including an investigation into its behavior at high pressure [13].

At $\sim$0.5 GPa, α-Li_3N transforms into a second layered hexagonal structure (β, $P6_3/mmc$) with BN-like honeycomb LiN layers [14]. In this structure, each nitrogen binds an additional lithium atom above and below the plane and adjacent LiN layers are shifted relative to one another, unlike the Li_2N layers in α-Li_3N. β-Li_3N is metastable at ambient pressure and is typically found mixed with the α-phase. It remains stable up to 35 GPa – the high-pressure limit of experiments on Li_3N to date. A second phase transition to a cubic structure - P43m at 37.9 GPa [13] or Fm3m at 27.6 GPa [15] - has been predicted. If it exists, the similarity of this phase those of other simple ionic cubic solids such as NaCl makes it an interesting study, particularly in light of its higher ionicity. Understanding the behavior of the unstable and highly charged N^{3-} ions under large compression will be particularly important.

In this paper, we present the first concrete experimental evidence that β-Li_3N indeed transforms to a cubic (Fm3m) structure which we will call γ-Li_3N in the pressure range of 36-45 GPa. This transformation resembles the graphite $\rightarrow$ diamond transition in many regards. It represents an increase in structural and bonding strength and isotropy, and is accompanied by a relatively large volume collapse and a significant widening of the electronic band gap. We find that γ-Li_3N is uniquely stable and highly compressible up to at least 200 GPa, making it a good candidate for an internal pressure standard.

Polycrystalline lithium nitride powder (99.5 % purity, CERAC, Inc) was loaded into a membrane diamond-anvil cell of LLNL design. Several diamond sizes were used to obtain an extended range of pressure up to 200 GPa. In the lower pressure experiments, argon was used as a pressure medium and internal pressure standard. For the high-pressure experiments, no pressure medium was used, and copper or ruby (Al_2O_3:Cr^{3+}) were included in the sample chamber as a pressure indicator. Despite non-hydrostatic conditions, we found the compression data

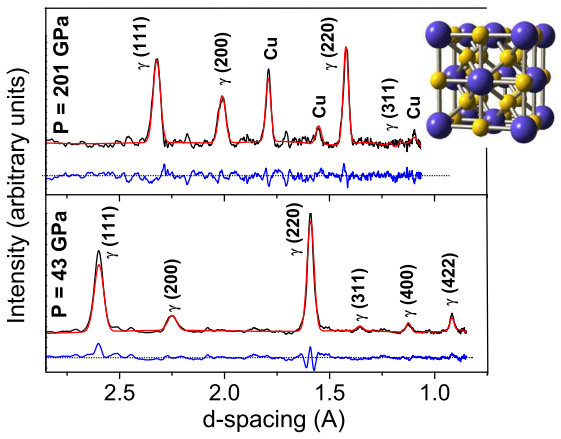

FIG. 1: Synchrotron x-ray diffraction spectra of γ-Li_3N at 43 and 201 GPa, with refined and difference patterns. Miller indices are noted based on the cubic (Fm3m) structure shown.

TABLE I: Comparison with previous results for β- and γ-Li_3N. Errors are from imperfect fits of the BM-EOS to data points - primarily a result of some non-hydrostaticity in the pressure cell in the experiment, causing strain in the sample. The γ-phase found in reference [13] is space group P43m.

		V_0 ($\frac{\AA^3}{atom}$)	B_0(GPa)	B_0'	$\frac{\Delta V}{V_0}$	P_T(GPa)
Exp.	β	8.6(.2)	71(19)	3.9(.9)	~8%	40(5)
	γ	7.7(.2)	78(13)	4.2(.2)		
Th.	β	8.61(.02)	68(3)	3.6(.1)	6.7%	40.4
	γ	7.79(.02)	73.1(.8)	3.85(.01)		
[13]	β	8.76	74(6)	3.7(.7)		
[13]	β	7.72	78.2	3.77	8%	37.9
	γ	7.02	82.8	3.84		
[15]	β	8.34				28(5)
	γ	7.61				
[14]	β	8.62				>10

did not differ significantly from that which was obtained under quasi-hydrostatic conditions. This is due to the high compressibility of Li_3N which will be discussed later. All samples were loaded in an argon environment as Li_3N is hygroscopic. High-pressure behavior of Li_3N was investigated by angle-dispersive powder x-ray diffraction (ADXD) at 16IDB and inelastic x-ray Raman scattering (XRS) at 16IDD of the High-Pressure Collaborative Access Team (HPCAT) beamlines at the Advanced Photon Source (APS). For the ADXD experiments, we used intense monochromatic x-rays (λ = 0.3683 or 0.4126 Å) microfocused to ~10 μm at the sample using a pair of piezo-crystal controlled bimorphic mirrors. The x-ray diffraction patterns were recorded on a high-resolution image plate detector (MARS 350) and analyzed with the FIT2D, XRDA and GSAS programs. For the XRS experiments, we used monochromatic x-rays (9.687 keV) focused to ~20 x 50 μm at the sample through an x-ray translucent Be gasket by a pair of 1 m-long Kirkpatrick-Baez focusing mirrors. Six spherically bent Si(660) single crystal analyzers (50 mm in diameter) were vertically mounted on a 870 mm Rowland circle to refocus inelastically scattered x-ray photons onto a Si detector (Amp Tek) at a scattering angle of 25° in a nearly back scattering geometry (Bragg angle of 88.6°). This configuration corresponds to a momentum transfer of q ~2.2 $Å^{-1}$. The overall system provides an energy resolution of ~1 eV.

At low pressures our x-ray data indicate a coexistence of α and β phase, consistent with the previous observation [13]. The mixture converts to a single phase of β-Li_3N near 0.5 GPa, which appears opaque. Between 35 and 45 GPa, we found that β-phase transforms to a new transparent phase, γ-Li_3N. Figure 1 shows the measured and refined diffraction patterns of γ-Li_3N at 43 GPa and 201 GPa, the maximum pressure achieved in the present study. The refinement was performed based on a cubic structure (Fm3m) with one formula unit per primitive fcc cell consisting of a rocksalt LiN lattice with the two additional lithium ions occupying the -43m (8c) sites, each tetrahedrally coordinated with 4 nitrogen ions.

The pressure-volume data for the β and γ phases and their 3rd order Birch-Murnaghan equation of state (BM-EOS) fits are shown in Figure 2, with fitting parameters summarized in Table I. The $\beta \rightarrow \gamma$ phase transition is accompanied by an 8% volume collapse and an increase in the coordination number for every atom. In the β phase, each N^{3-} ion is surrounded by 11 Li^+ ions (three in the hexagonal planes at 1.85 Å, two above and below the plane at 1.90 Å and six in trigonal prismatic coordination at 2.08 Å at the transition). In the γ phase, 14 Li^+ ions surround N^{3-}, eight tetrahedrally coordinated with N at 1.95 Å and six octahedrally at 2.25 Å. Across the phase transition there is no discontinuity in the nearest-neighbor nitrogen atom distance (~3.23 Å), and the nearest nitrogen-lithium distance even increases slightly. The significant increase in packing without a decrease in distance between highly charged nitrogen ions makes the γ phase highly preferred at high pressures. The more populated and symmetric distribution of lithium ions serves to effectively shield the highly charged nitrogen ions from one another and even potentially to compress their ionic radii [16], thus stabilizing the cubic structure up to very large lattice constant reduction.

The compressibility of γ-Li_3N rivals other common and highly compressible closed-shell cubic solids as seen in the inset of Figure 2. Values for bulk modulus were obtained as a function of pressure by fitting to the pressure-volume data with a BM-EOS modified relative to some non-ambient-pressure reference volume [17]. The fitting parameters were then used to calculate values for bulk modulus over a wide-range of pressures. The results clearly show that γ-Li_3N is harder than argon, but softer than MgO and even NaCl above 100 GPa. The distinct lack of broadening in the measured ADXD (seen at 201 GPa

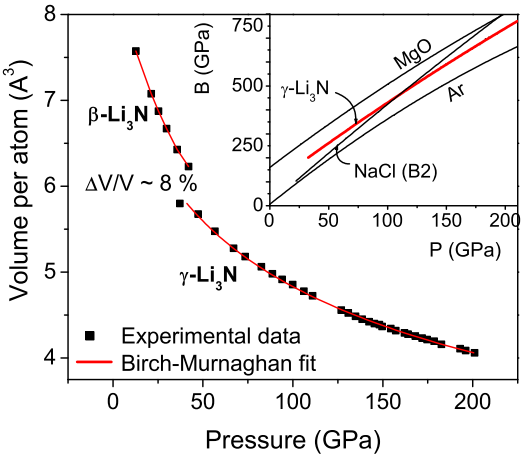

FIG. 2: Equation of state of β- and γ-Li_3N. In the inset, the high pressure Bulk Modulus of γ-Li_3N is compared to other common highly compressible materials.

in Figure 1) even in the absence of a pressure medium further signifies high compressibility of the cubic phase.

The differences in crystal structure of γ-Li_3N from the α- and β- phases suggest that there will also be distinct differences in electronic structure. To validate this conjecture, we have carried out XRS experiments at the nitrogen K absorption edge. The most distinct features of the XRS spectrum (shown in black in Figure 3) are a narrow near edge peak near 397 eV and a main edge near 403 eV, both of which change under pressure. The near edge, arising from low-lying conduction bands, decreases in intensity in each phase and has completely disappeared in the cubic phase, in correlation with the decreasing structural anisotropy. One consequence of this anisotropy in the hexagonal phases is high compressibility parallel to the c-axis. Upon application of pressure in this study, the c/a ratio underwent a marked decrease in the β-phase and Dovesi states that the α phase appears even more compressible along c [2]. Thus, the near edge feature may be seen as a signature of the presence of more weakly interacting ions perpendicular to the a-b planes - a consequence of the large empty spaces between the planes. This is consistent with previous observations of a large and anisotropic electronic polarizability of the N^{3-} ions in the hexagonal structure [18, 19]. The main edge would then describe the ion interactions within the plane. The higher energy of these unoccupied states indicates that the conduction bands are less accessible due to the relatively smaller interstitial space in which to house itinerant electron states within the planes. The shift to higher energy of all peaks in each subsequent phase transition reflects a further decrease in interstitial space in all directions.

In order to explain the observed structural and spectral changes, we have also performed first-principles elec-

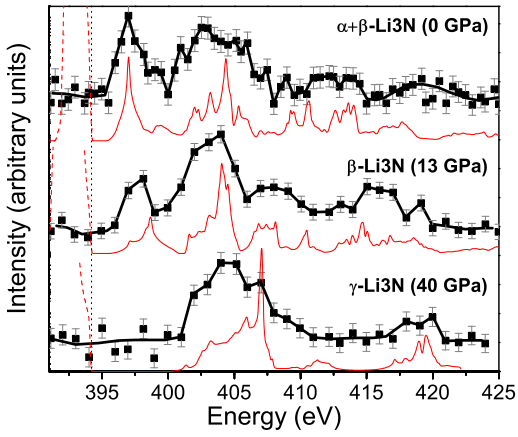

FIG. 3: XRS of α-, β-, and γ-Li_3N shown in black and error bars estimated as the square root of the counts. Nitrogen 2p projected DOS are shown in red beneath experimental curves, offset by 394.2 eV with occupied valence states as dashed lines, and vertical line representing the Fermi energy.

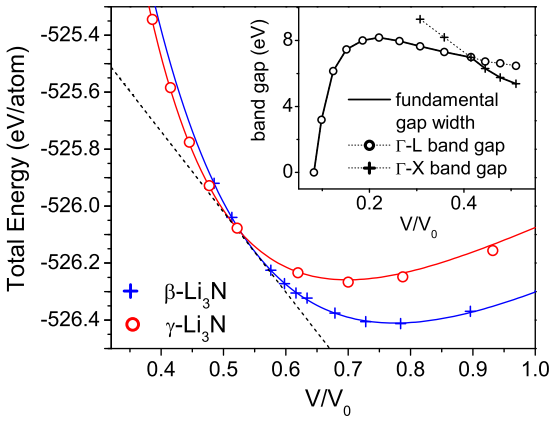

FIG. 4: Calculated EOS of β- and γ-Li_3N. The slope of the dotted line represents the transition pressure. The collapse of the electronic band gap under pressure is shown in the inset. V_o is the atomic volume at ambient pressure.

tronic structure calculations. Because of the large six-fold compression carried out in these calculations, we used two methods for comparison: full-potential linearized augmented plane-waves (LAPW) as implemented in WIEN2k code [20] within the Generalized Gradient Approximation [22] and a full-potential nonorthogonal local-orbital minimum basis bandstructure scheme [21], within the local spin-density approximation (LSDA) [23]. We found good agreement between these two results. Figure 4 summarizes total energy calculations on the β and γ phases at various compressions and their BM-EOS fits (lines). The calculated equilibrium volumes, bulk moduli, and transition pressure are all in good agreement with experimental values (see Table I), giving us confidence in the theoretical models employed.

Using this model, we have calculated the projected nitrogen p density of states (pDOS) to compare with the XRS data in Figure 3. Within the dipole approximation, the relative intensities of the XRS spectrum should be proportional to the pDOS and the squared dipole transition-matrix element. If the matrix element does not have a sharp energy dependence, the XRS and pDOS should be rather closely related, which is clearly the case in Figure 3. This agreement reveals that the electronic states observed in the XRS study can be well understood as 1s $\rightarrow$ 2p transitions, and also indicates that core-hole-electron interactions (excitons) have a lesser effect on these spectra than often observed [24–26]. It further reveals that the structural anisotropy responsible for the existence of the near edge peak leads to the presence of low energy conduction bands and results in a smaller electronic band-gap in the hexagonal phases than in the cubic phase. Experimentally, such a band-gap increase is evident from an optical change from opaque β to transparent γ phase. Since these low-lying conduction states come from weak binding of electrons in a direction

perpendicular to the hexagonally-bonded a-b planes, one may expect to observe some amount of delocalized charge in the interstitial regions outside of the planes, which has indeed been indicated [1]. In the cubic phase, then, we expect more localized and symmetric charge distributions around the nitrogen atoms, making them even closer to the ideal ionic state (N^{3-}) and explaining the insulating character and high stability of this phase. In spite of a similarity between these transitions and the 1s to π^* and σ^* transitions in graphite-diamond and boron nitride, an examination of the p_x, p_y and p_z character in Li_3N reveals that the near edge peak has a significant $p_{x,y}$ component in addition to p_z, and the main edge composition (primarily Li and N p character) does not suggest any significant hybridization between Li s and N p orbitals as is the case between B s and N p states in boron nitride.

Our calculated electronic structures further reveal that, upon decreasing unit cell volume, the (indirect) band-gap continues to increase up to a calculated pressure of ∼760 GPa ($V/V_o = 0.22$) before beginning to collapse (see Figure 4, inset). Band-gap closure does not occur until ∼8 TPa ($V/V_o = 0.08$), which will be a lower limit, based on the tendency of the local density approximation to underestimate the band gap. This high metallization pressure places γ-Li_3N in the same family as other closed-shell, cubic insulating solids such as Ne, MgO and NaCl, which metallize near 134 TPa, 21 TPa and 0.5 TPa, respectively [27–29]. An examination of metallization in these materials reveals a trend that the states with smaller ℓ (orbital character) increase in energy with respect to larger ℓ because they are more extended and hence more greatly affected by pressure, so metallization occurs as a result of overlap between valence sp states and conduction d states [30]. Neon is isoelectronic to N^{3-}, and its metallization pressure is remarkably high because there is no 2d band, so that the overlap must occur between 2sp valence states and the much higher energy 3d conduction states. Li_3N is more complex, however, as the low-lying conduction bands have primarily Li(2p) character, with a negligibly small amount of N d character at band closure. Therefore, the phenomenon in Li_3N is more of an interspecies metallization which perhaps explains its 20-times lower metallization pressure than predicted for the intraspecies metallization in neon.

In summary, we have provided a coherent picture of the structural and spectral changes associated with a graphite-diamond-like phase transition in Li_3N, understood here for the first time. The high-pressure cubic phase has several interesting and unique properties including unusually high phase stability to pressures exceeding 200 GPa, high compressibility rivaling commonly used pressure media such as NaCl, and also an ultra-high metallization pressure that makes it one of the most difficult materials to metallize that we know of.

We would like to acknowledge D. Kasinathan and J. Kuneš for useful discussions during this investigation. Use of the HPCAT facility was supported by DOE-BES, DOE-NNSA (CDAC), NSF, DOD-TACOM, and the W. M. Keck Foundation. We thank HPCAT beamline scientist M. Somayazulu for technical assistance. This work has been supported by the LDRD-04-ERD-020, PDRP and SEGRF programs at the LLNL, University of California, U.S. DOE No. W-7405-ENG-48, by the SSAAP, DOE DE-FG03-03NA00071, and by the NSF, ITR 031339.

[1] G. Kerker, Phys. Rev. B **23**, 6312 (1981)
[2] R. Dovesi et al., Phys. Rev. B **30**, 972 (1984).
[3] E. Zintl and G. Brauer, Z. Elektrochem, **41**, 102 (1935).
[4] A. Rabenau and H. Schulz, J. Less Common Metals **50**, 155 (1976); A. Rabenau, Solid State Ionics **6**, 277 (1982).
[5] M. L. Wolf, J. Phys. C: Solid State Phys. **17**, L285 (1984).
[6] J. Sarnthein et al., Phys. Rev. B **53**, 9084 (1996).
[7] E. Bechtold-Schweickert et al., Phys. Rev. B **30**, 2891 (1984).
[8] P. Chen et al., Nature **420**, 302 (2002).
[9] T. Ichikawa et al., J. Alloys Compd. **365**, 271 (2004).
[10] Y. H. Hu et al., Ind. Eng. Chem. Res. **44**, 1510 (2005).
[11] Y. Nakamori et al., Appl. Phys. A: Mat. Sci. Process. **80**(1): 1 (2005).
[12] Y Xie et al., Science **272**, 1926 (1996).
[13] A. C. Ho et al., Phys. Rev. B **59**, 6083 (1999).
[14] H. J. Beister et al., Angew. Chem. Int. Ed. **27**, 1101 (1988).
[15] J. C. Schön et al., J. Mater. Chem. **11**, 69 (2001).
[16] M. W. Wilson et al., J. Chem. Phys. **104**, 8068 (1996).
[17] N. Sata et al., Phys. Rev. B **65**, 104114 (2002).
[18] H. R. Chandrasekhar et al., Phys. Rev. B **17**, 884 (1978).
[19] W. Kress et al., Phys. Rev. B **22**, 4620 (1980).
[20] P. Blaha et al., *WIEN2k*, Karlheinz Schwarz, Techn. Universität Wien, Wien, 2001.
[21] K. Koepernik and H. Eschrig, Phys. Rev. B **59**, 1743 (1999).
[22] J. P. Perdew, K. Burke, and M. Ernzerhof, Phys. Rev. Lett. **77**, 3865 (1996).
[23] J. P. Perdew and Y. Wang, Phys. Rev. B **45**, 13244 (1992).
[24] R. Buczko et al., Phys. Rev. Lett. **85**, 2168 (2000).
[25] A. Soininen, Academic Dissertation, University of Helsinki (2001).
[26] E. L. Shirley, Phys. Rev. Lett. **80**, 794 (1998); E. L. Shirley et al., J. of Electron Spectrosc. Relat. Phenom. **114-116**, 939 (2001).
[27] J. C. Boettger, Phys. Rev. B **33**, 6788 (1986).
[28] A. R. Oganov, M. J. Gillan, G. D. Price, J. Chem. Phys. **118**, 10174 (2003).
[29] J. L. Feldman et al., Phys. Rev. B **42**, 2752 (1990).
[30] A. K. McMahan, Physica **139 & 140B**, 31 (1986); A. K. McMahan and R. C. Albers, Phys. Rev. Lett. **49**, 1198 (1982).